NASA Technical Memorandum 84616 NASA-TM-84616 19830012643

TRANSONIC PRESSURE DISTRIBUTIONS ON A RECTANGULAR SUPERCRITICAL WING OSCILLATING IN PITCH

RODNEY H. RICKETTS, MAYNARD C. SANDFORD
DAVID A. SEIDEL AND JUDITH J. WATSON

MARCH 1983

National Aeronautics and
Space Administration

Langley Research Center
Hampton, Virginia 23665

TRANSONIC PRESSURE DISTRIBUTIONS ON A RECTANGULAR SUPERCRITICAL WING OSCILLATING IN PITCH

Rodney H. Ricketts Maynard C. Sandford David A. Seidel and Judith J. Watson
NASA Langley Research Center
Hampton, Virginia 23665

Abstract

Steady and unsteady aerodynamic data were measured on a rectangular wing with a 12 percent thick supercritical airfoil mounted in the NASA Langley Transonic Dynamics Tunnel. The wing was oscillated in pitch to generate the unsteady aerodynamic data. The purpose of the wind-tunnel test was to measure data for use in the development and assessment of transonic analytical codes. The effects on the wing pressure distributions of Mach number, mean angle of attack, and oscillation frequency and amplitude were measured. Results from the newly-developed XTRAN3S program (a non-linear transonic small disturbance code) and from the RHOIV program (a linear lifting surface kernel function code) were compared to measured data for a Mach number of 0.7 and for oscillation frequencies ranging from 0 to 20 Hz. The XTRAN3S steady and unsteady results agreed fairly well with the measured data. The RHOIV unsteady-result agreement was fair but, of course, did not predict shock effects.

Symbols

b	wing span, ft (4.0)
c	wing chord, ft (2.0)
cg	wing center of gravity
C_L	total wing lift coefficient
C_p	pressure coefficient, $(p-p_\infty)/q$
EI	bending stiffness, lb-in^2
f	wing pitch frequency, Hz
GJ	torsional stiffness, lb-in^2
k	reduced frequency, $c\omega/2V$
M	free-stream Mach number
p	transducer local static pressure, lb/in^2
p_∞	free-stream static pressure, lb/in^2
q	free-stream dynamic pressure, lb/in^2
t/c	thickness-to-chord ratio
V	free-stream velocity, ft/sec
x/c	fractional chord
α	mean angle of attack, deg
$\Delta\alpha$	pitch oscillation amplitude, deg
ΔC_p	lifting pressure coefficient (difference between lower- and upper-pressure coefficients)
$\lvert\Delta C_p\rvert$	magnitude of lifting pressure coefficient
n	fractional span, y/b
ϕ	phase between lifting pressure and wing pitch angle, deg (positive for pressure leading motion)
ω	circular frequency, rad/sec

Introduction

In recent years NASA Langley Research Center has had a program for measuring unsteady aerodynamic data in the transonic regime for the purposes of assisting analytical code development and providing a data base for active controls design. Two models previously tested in the 16-foot Transonic Dynamics Tunnel (TDT) are a clipped delta wing[1] and a high-aspect-ratio transport wing[2]. The delta wing, which had a circular-arc airfoil, was oscillated in pitch at various mean angles of attack. A trailing-edge control also was oscillated to generate unsteady aerodynamic data. The transport-type wing with a supercritical airfoil had five leading-edge and five trailing-edge control surfaces of which some were oscillated independently and in pairs about various mean control surface angles. The static angle of attack of the transport-type wing was varied to allow data acquisition at cruise lift conditions.

Additional tests have been completed on a third wing--a rectangular wing having a supercritical airfoil. This particular wing (a simple planform geometry) was tested for the purpose of aiding in the development and preliminary assessment of new analytical transonic codes such as XTRAN3S[3,4]. The results obtained from this test provide the database desired for extension of two-dimensional flows to three-dimensional flows. This paper describes this recent test of the rectangular wing, presents measured data, and correlates these experimental results with theoretical results.

Wing Configuration

A photograph of the wing installed in the TDT is shown in Fig. 1. The wing is attached to a shaft that extends through a splitter plate mounted off the wind-tunnel wall so that the wing root is outside the wall boundary layer. The shaft is connected to a hydraulic rotary actuator that oscillates the wing in pitch.

Geometry

The details of the planform and airfoil shape are shown in Fig. 2. The unswept wing has a rectangular planform with a 2-ft chord and a 4-ft span (panel aspect ratio of 2.0). The airfoil is a 12-percent thick (t/c = 0.12)

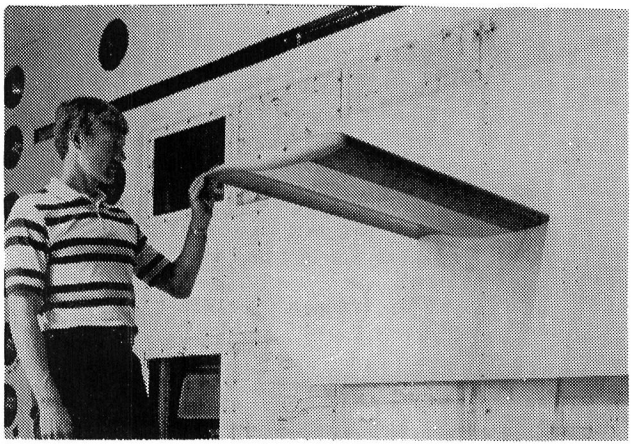

Fig. 1 Wing mounted in TDT test section.

supercritical shape with a two-dimensional design Mach number of 0.8 and design lift coefficient of 0.6. The airfoil was derived from an 11-percent thick airfoil[5] by increasing the thickness-to-chord ratio and the trailing-edge thickness. The wing tip was formed by connecting the upper and lower surfaces with semi-circular arcs. The wing pitch axis is located at the 0.46 fractional chord. This location was chosen to maximize performance of the actuator (considering both aerodynamic and inertia loads).

Construction

The wing was constructed in three sections as shown in Fig. 3 to allow easy access to the instrumentation located within the wing. The wing center box section was made from aluminum halves (upper and lower) that were permanently bonded and bolted together. The leading- and trailing-edge sections were made of light-weight Kevlartt and balsawood sandwich material to

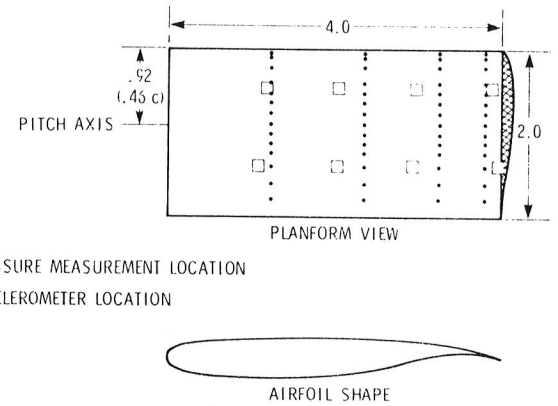

Fig. 2 Planform view and airfoil shape of wing. Dimensions in feet.

ttKevlar: Registered trademark of E. I. du Pont de Nemours & Co., Inc. Use of trade names does not constitute an official endorsement, either expressed or implied, by NASA.

minimize the pitch moment of inertia of the wing assembly. The leading- and trailing-edge sections were attached to the center box section at 0.23 and 0.69 fractional chords, respectively.

Instrumentation

Wing instrumentation consisted of 126 differential pressure transducers, eight accelerometers, and one potentiometer. The transducers were mounted at four spanwise stations to measure both static and dynamic pressures along chordwise rows (see Fig. 2) on the upper and lower surfaces. Each transducer was referenced to the tunnel static pressure. In the center box section, the transducers were mounted flush to the surface (in situ). For the leading- and trailing-edge sections, the transducers were located in the joint area between the sections (see Fig. 3) and were connected to orifices at the section surfaces via tubes that had equal length and diameter. This arrangement alleviated the problems associated with in situ mounting in the thin trailing-edge areas and to

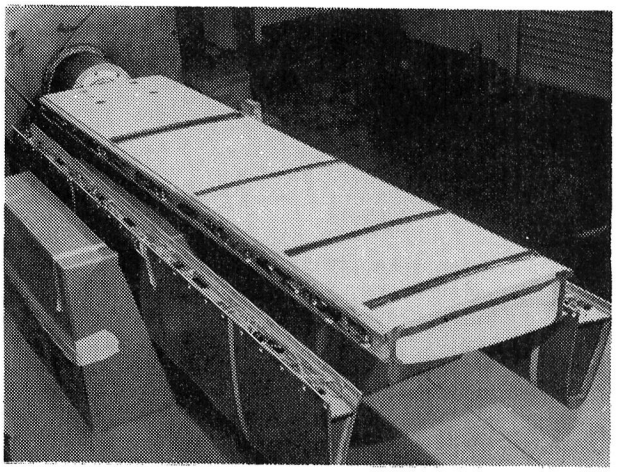

Fig. 3 Pressure instrumentation in leading- and trailing-edge attachment areas.

enable the transducers to be mounted closer to the pitch axis and thereby reduce the accelerations that they experience. This tube technique for measuring unsteady pressures was first introduced by Tijdeman[6] and is often called the Dutch matched-tubing method. A fifth row of matched-tubing transducers was installed with orifices adjacent to the inboard row of in situ transducers in the center box section. Data obtained from these "colocated" in situ and matched-tubing transducers were used to measure (or, calibrate) the tube effects on the unsteady pressure magnitude and phase. The results of the calibration were then applied to the pressure data measured on the leading- and trailing-edge sections. The accelerometers were used to measure wing dynamic motion and were mounted along the front and rear edges of the center box section. A potentiometer connected to the actuator shaft was used to measure both static and dynamic motion of the wing root.

Structural Properties

Laboratory measurements were made to determine the weight, stiffness, and vibration properties of the assembled wing with instrumentation installed. The measured quantities are presented in Table 1. These values are within design objectives to allow oscillations of the wing with an existing actuator to frequencies up to 20 Hz at an amplitude of ±1 deg without significant wing structural deformation. (Note that the wing fundamental elastic frequency is about 35 Hz.) In addition, the airfoil coordinates were measured at five span stations and were shown to be within 0.02 in of the design values.

Table 1 Measured structural properties of wing.

WEIGHT	54 lb
CG LOCATION, x/c	0.44
η	0.41
PITCH INERTIA	1050 lb-in.^{2}
EI	75×10^6 lb-in.^{2}
GJ	100×10^6 lb-in.^{2}
FUNDAMENTAL FREQUENCY.	34.8 Hz

Wind Tunnel

The Langley Transonic Dynamics Tunnel (TDT) is a closed-circuit continous-flow tunnel which has a 16-ft square test section with cropped corners and slots in all four walls. Mach numberand dynamic pressure can be varied simultaneously, or independently, with either air or Freontt used as a test medium. All data presented in this report were obtained using a Freon medium.

Data Acquisition and Reduction

Data from the model instrumentation were acquired using the TDT real-time data acquisition system[7] and reduced in a "near real-time" manner.

Steady (static) pressures were measured using the differential pressure transducers installed in the wing. One thousand samples of data at a rate of 300 samples per second were averaged for each transducer to determine mean values of pressure coefficient. Data were acquired simultaneously from all the transducers at a given span station.

Unsteady (dynamic) pressures were calculated from transducer time-history data that were measured at a rate of 300 samples per second and recorded on digital tape. A discrete Fourier transform of 75-100 cycles of the data (a minimum of 15 samples per cycle) was used to determine the first harmonic pressure coefficient magnitude and phase in relation to the pitch position of the wing root. The magnitude and phase measurements from transducers using the matched-tubing method were determined using transfer functions derived from calibration data from corresponding in situ and matched-tubing transducers. In addition, the wing motion at the root was determined from discrete Fourier transforms of time-history data that were measured using the potentiometer. Aeroelastic deformations of the wing during the pressure data acquisiton were determined from discrete Fourier transforms of time-history data measured using the accelerometers.

Test Results and Discussion

Steady and unsteady pressures were measured for a large number of test conditions in the TDT as illustrated in Fig. 4 which shows the wing total lift coefficient plotted against Mach number for angles of attack ranging from -1 to 7 deg. For the unsteady-data points (solid symbols) in Fig. 4, the wing oscillation frequencies were 5, 10, 15 and 20 Hz. Some representative results obtained during these tests are presented in this section. The Reynolds number based on the chord length is four million for all data presented.

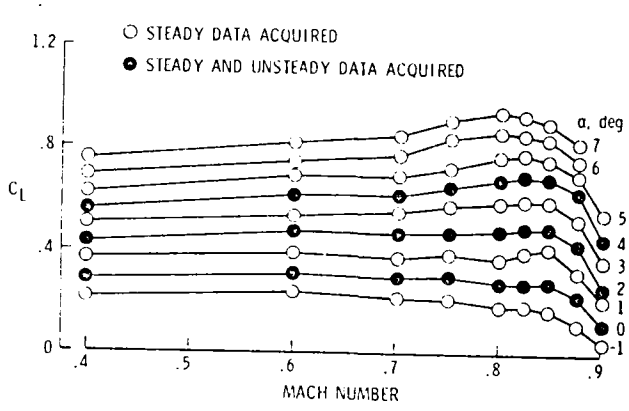

Fig. 4 Total wing lift coefficient for various angles of attack plotted against Mach number.

Steady Results

Upper- and lower-surface steady pressure distributions at the four spanwise stations are shown in Fig. 5 for a Mach number of 0.825 and an angle of attack of 4 deg. (This is close to the 2-D design condition for the airfoil.) At the inboard sections, typical supercritical flow is present on the upper surface--namely, a rather flat pressure region followed by a weak shock far aft (0.50 to 0.60 fractional chord) on the wing. However, for sections farther out on the wing this shock is farther forward toward the leading edge as a result of the effects of the wing tip. At the wing tip the shock is located at about the 0.10 fractional chord. The pressure distributions on the lower surface are not affected by the presence of the wing tip.

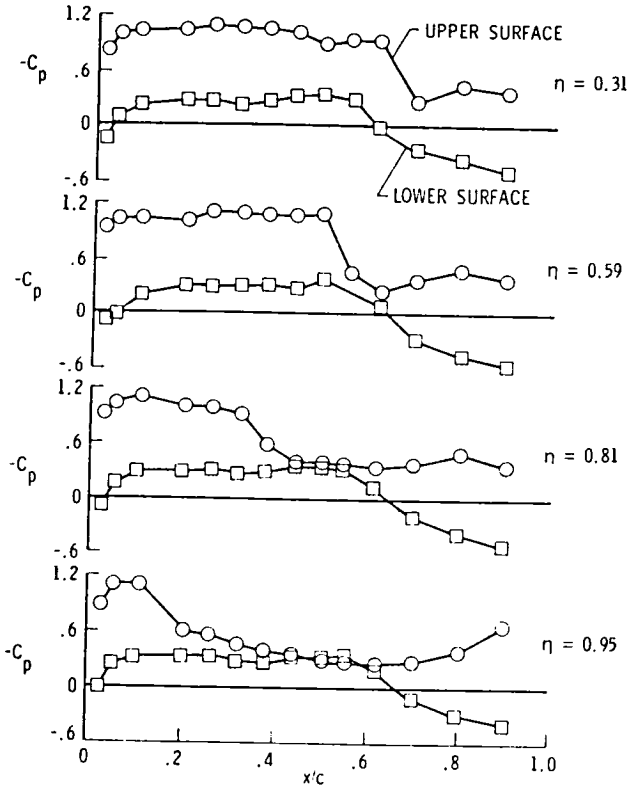

Fig. 5 Steady pressure distributions at four spanwise stations. M = 0.825, α = 4 deg.

Unsteady Results

Some of the unsteady pressure distributions measured during the tests are summarized in this section. The results are presented in terms of the magnitude and phase of the lifting pressure coefficient ($|\Delta C_p|$ and ϕ, respectively). On the figures presented in this section, curves are faired through the data points in the region of the shock to show trends and estimated peak-pressure (shock) locations.

Span Effects.- Pressure distributions at the four spanwise stations are shown in Fig. 6 for a mean angle of attack of 4 deg and a Mach number of 0.825. The oscillation amplitude and frequency are ±1 deg and 10 Hz (k=0.15), respectively. The pressure peaks, which are indicative of dynamic shock motion, vary significantly across the wing span. By comparison with the steady data (Fig. 5), it is seen that the pressure peaks are located near the same chordwise positions as the upper surface static shocks. The unsteady shock strength decreases nearer the tip region. The phase results in Fig. 6 show that the pressure is generally lagging the wing pitch motion (negative phase) forward of the pitch axis (0.46 fractional chord) and leading it aft of the axis. For the two inboard stations where the shocks are located aft of the pitch axis, the lag-to-lead phase shift occurs aft of the shock.

Mach Number Effects.- Pressure distributions at the inboard station (0.31 fractional span) are shown in Fig. 7 for seven Mach numbers ranging from 0.4 to 0.85. The wing mean angle of attack is 2 deg. The oscillation amplitude and frequency are +1 deg and 10 Hz, respectively (k ranges from 0.31 at 0.4 Mach number to 0.15 at 0.85 Mach number). The pressure peak is located at the leading edge for the low subsonic Mach numbers but rapidly moves aft as the Mach number increases. At a Mach number of 0.85 the estimated shock location is near the three-quarter chord. This is better shown in Fig. 8 where the estimated shock location in fractional chord is shown plotted against Mach number. In this figure it is seen that the shock begins to move aft rapidly as the Mach number is increased above 0.6. For the most part, the phase data (see Fig. 7) show that the pressures lag the motion ahead of the shock and lead behind the shock.

Mean Angle-of-Attack Effects.- Pressure distributions at the inboard station (0.31 fractional span) are shown in Fig. 9 for three mean angles of attack at a Mach number of 0.825. The oscillation amplitude and frequency are ±1 deg and 10 Hz (k = 0.15), respectively. The results show that, as the angle of attack increases, the shock moves aft on the wing, and the pressures ahead of the shock decrease considerably in magnitude. The phase data show that the pressures lag the motion ahead of the shock and lead the motion aft of the shock. For increasing mean angles of attack, the phase angles ahead of the shock increase slightly.

Oscillation Frequency Effects.- Pressure distributions at the inboard chord (0.31 fractional span) are shown in Fig. 10 for seven oscillation frequencies ranging from 2 to 20 Hz (k = 0.03 to 0.31) and an oscillation amplitude of ±1 deg. The Mach number and mean angle of attack are 0.8 and 2 deg, respectively. The results show that the frequency effect is large for both the magnitude and phase. As the

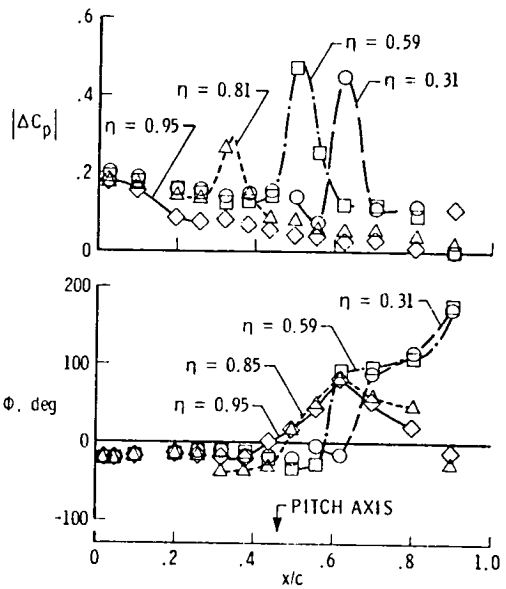

Fig. 6 Effects of span on unsteady pressure distributions at four spanwise stations. M = 0.825, α = 4 deg, f = 10 Hz, Δα = ±1 deg.

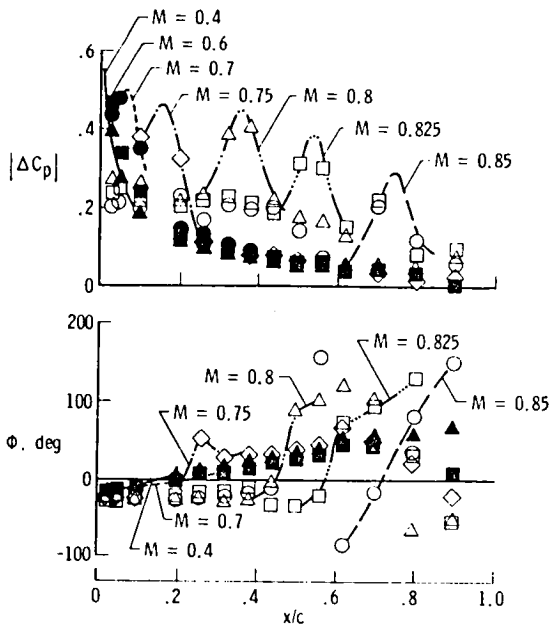

Fig. 7 Effects of Mach number on unsteady pressure distribution at $\eta = 0.31$. $\alpha = 2$ deg, f = 10 Hz, $\Delta\alpha = \pm 1$ deg.

frequency of oscillation increases, generally the magnitude of the pressure decreases forward of the pitch axis and increases behind the axis. The shock at approximately the 0.35 fractional chord coincides with the steady-state shock location and appears to decrease in strength as the frequency increases. The phase results show that the pressures lag the motion ahead of the shock and lead the motion behind the shock. The phase angle generally decreases (pressure lags the motion) as the frequency increases. This effect is more pronounced aft of the pitch axis.

Oscillation Amplitude Effects.- Pressure distributions for the inboard chord (0.31 fractional span) are shown in Fig. 11 for three oscillation amplitudes ranging from 0.5 to 1.5 deg and an oscillation frequency of 10 Hz (k = 0.16).

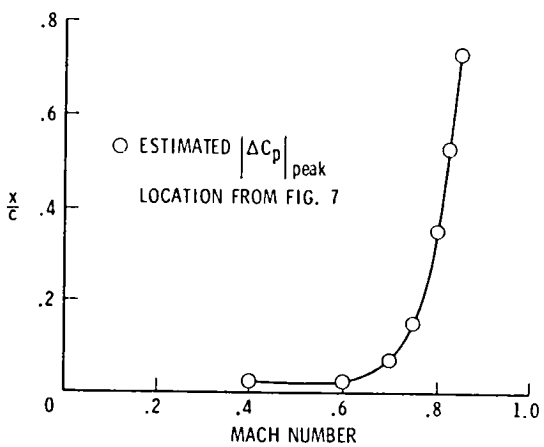

Fig. 8 Effect of Mach number on estimated shock location in fractional chord. $\alpha = 2$ deg, f = 10 Hz, $\Delta\alpha = \pm 1$ deg.

The Mach number and mean angle of attack are 0.8 and 3.3 deg, respectively. In the figure the pressure magnitudes are normalized by the oscillation amplitudes and show no appreciable difference either forward or aft of the shock for the three cases. Therefore, in these regions, it follows that the pressure magnitude increases linearly as the motion amplitude is increased in the range 0.5 to 1.5 deg. In the vicinity of the pressure peak there are differences in the data which indicate magnitude non-linearities in this region. No effect of oscillation amplitude is seen in the pressure phase data.

Comparison of Measured and Calculated Results

Unsteady pressure calculations were made with two theoretical programs, and the results are compared with measured data. One program is the newly developed XTRAN3S[3,4] which is a three-dimensional non-linear transonic code which uses finite difference methods to derive a

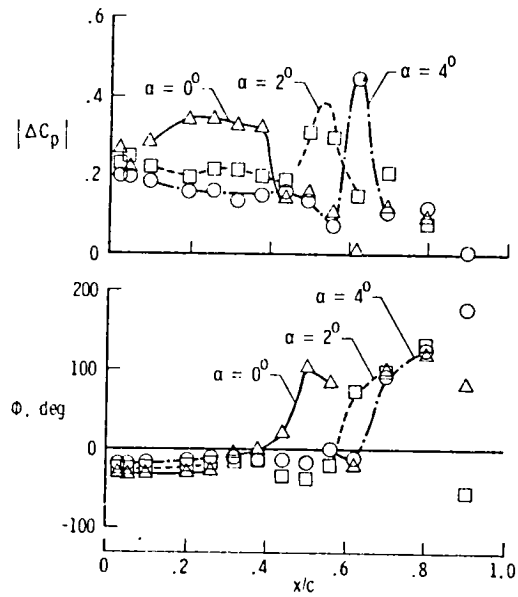

Fig. 9 Effects of mean angle of attack on unsteady pressure distribution at $\eta = 0.31$. M = 0.825, f = 10 Hz, $\Delta\alpha = \pm 1$ deg.

time-accurate solution from the small disturbance potential equation. This code does not include the effects of viscosity. These XTRAN3S results were obtained using the following to improve the accuracy and agreement with the measured data: (1) a revised grid arrangement[8], and (2) small disturbance equation coefficients derived by the National Aerospace Laboratory of the Netherlands[9]. The other program used for the unsteady pressure comparisons is RHOIV[10] which is a linear subsonic lifting surface kernel function theory based on the acceleration potential. In addition to the unsteady comparisons, steady pressure comparisons are made using the XTRAN3S program.

Comparisons are made for calculated and measured results at a Mach number of 0.7. The

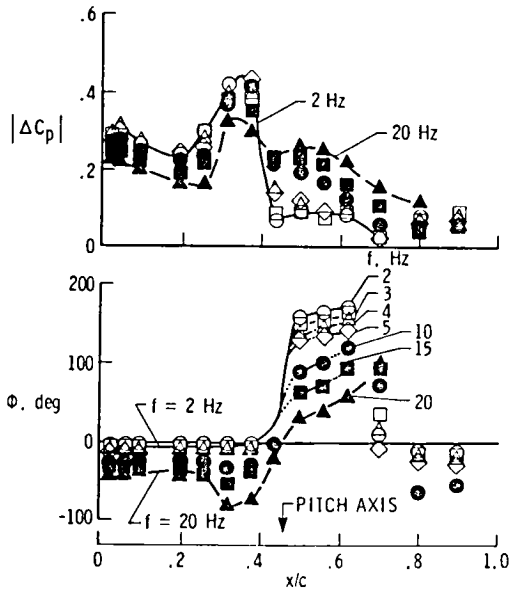

Fig. 10 Effects of frequency on unsteady pressure distribution at η = 0.31. M = 0.8, α = 2 deg, $\Delta\alpha$ = $\pm$1 deg.

mean angle of attack is 2 deg. The oscillating amplitude and frequency range for the unsteady data are $\pm$1 deg and 5 to 20 Hz (k = 0.09 to 0.36), respectively. Rigid pitch motions were used in the unsteady calculations. For XTRAN3S results, the measured wing coordinates were used.

Steady Results

Comparisons of steady upper- and lower-surface pressure distributions at the four span stations are shown in Fig. 12. The comparisons are good over most of the wing. The XTRAN3S program accurately predicted at all spanwise stations both the upper-surface pressures aft of the shock and the lower-surface pressures in the mid-chord region. The results deviate somewhat in the leading-edge region and on the lower surface near the trailing edge. The comparisons in these regions may possibly be improved by including viscous effects in the code and by decreasing the grid spacing for the calculations in this region to account for the bluntness of this airfoil (see Fig. 2). Analysis of this airfoil with the two-dimensional full potential program[11] indicate that including viscous effects at this condition tends to raise the lower-surface pressures in the leading-edge region as a result of a de-cambering effect of the boundary layer in the aft portion of the airfoil. A finer grid may improve the upper-surface pressure-peak definition near the leading edge.

Calculations for a Mach number of 0.825 (not shown here) showed significantly poorer agreement than the results for 0.7 Mach number. For this case the upper surface-shock was calculated to be near the trailing edge rather than located as shown in Fig. 5. Again, the two-dimensional program indicated that inclusion of viscosity in the solution causes the shock to move forward nearer its proper location (approximately 0.6 fractional chord at the inboard spanwise station).

Unsteady Results

Upper- and Lower-Surface Pressure Comparison.- Unsteady upper- and lower-surface pressure distributions from measurements and XTRAN3S calculations are shown in Fig. 13 at a fractional span of 0.59 and an oscillation amplitude and frequency of +1 deg and 10 Hz (k = 0.18), respectively. The agreement of the pressure magnitudes is good over the aft three-quarters of the chord for both the upper- and lower- surface data. In the leading-edge region near the shock, the agreement is not as good. In this region XTRAN3S under predicted the magnitudes. The phase agreement is good over the forward three-quarters of the chord and degrades significantly near the trailing edge. No explanation for this disagreement is apparent.

Spanwise Pressure Comparison.- Unsteady lifting pressure distributions at the four spanwise stations are shown in Fig. 14. The comparison includes both measured data and results from XTRAN3S and RHOIV. The XTRAN3S program predicted fairly well the pressure magnitudes at all spanwise stations in the region aft of the

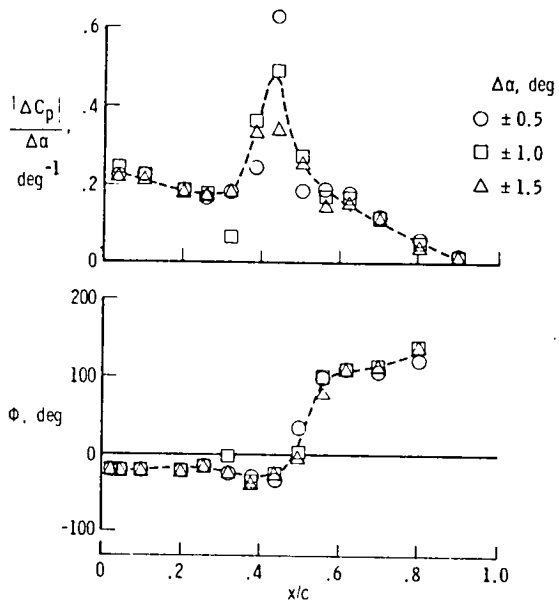

Fig. 11 Effects of oscillation amplitude on unsteady pressure distribution at η = 0.31. M = 0.8, α = 3.3 deg, f = 10 Hz.

shock (located near the leading edge). In the region of the shock the calculations over predicted the leading-edge pressures at the inboard station and under predicted those pressures at the outboard stations. The phase agreement is good over the forward two-thirds ofthe chord at the outboard two stations. The phase calculations at the two inboard stations are affected by the over-predicted leading-edge shock. The phase agreement is not good near the trailing edge. In this region the measured lifting-pressure phases show a strong influence of the lower-surface-pressure phase (see Fig. 13). The

RHOIV results are presented for 0.31, 0.59, and 0.81 fractional span stations. The pressure-magnitude agreement is fairly good over the aft two-thirds of the chord. However, at all spanwise stations the magnitude is under predicted in the forward half of the wing and over predicted in the aft portion of the wing. The leading-edge shock, of course, is not predicted by the linear theory. The phase agreement is good over the forward two-thirds of the wing and, in most cases, is better than the XTRAN3S agreement. Similar to the XTRAN3S results, the phase agreement near the trailing edge is not good.

Frequency Comparison.- Unsteady lifting pressure distributions at a fractional span of 0.59 are shown in Fig. 15 for oscillation frequencies of 5, 10, 15, and 20 Hz (k = 0.09 to 0.36). The comparison includes measured data and results from both XTRAN3S and RHOIV. In general, the XTRAN3S agreement is fairly good for both the phase and magnitude data. For these cases the strength of the shock at the leading edge is best predicted at the lowest frequency. At higher frequencies the shock strength is under predicted. The phase agreement is best at the two higher frequencies where the measured data do not have the monotonically-increasing trend reversed near the trailing edge. The RHOIV magnitude agreement is fairly good in the aft two-thirds of the chord at all frequencies. The phase agreement in the forward two-thirds of the chord is good and improves as the frequency decreases.

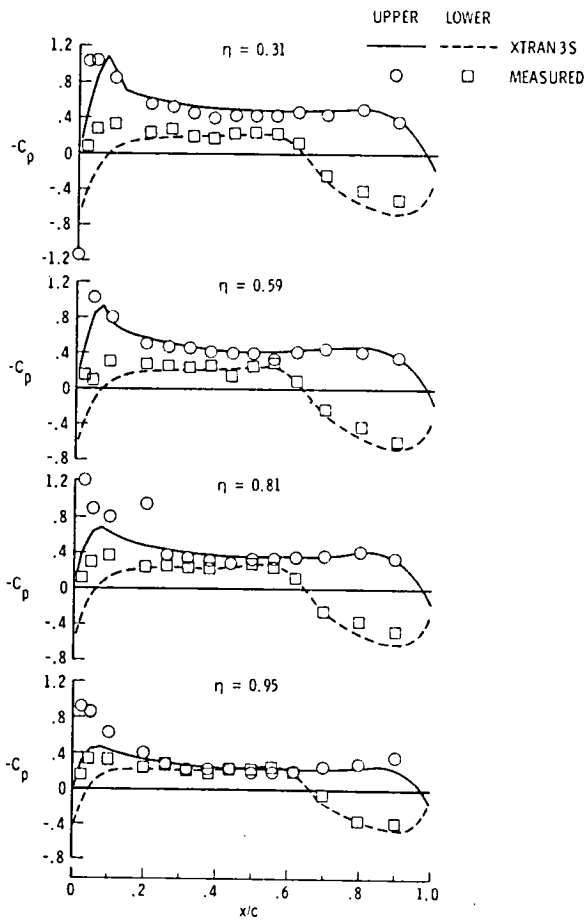

Fig. 12 Spanwise comparison of measured and calculated steady pressure distributions. M = 0.7, α = 2 deg.

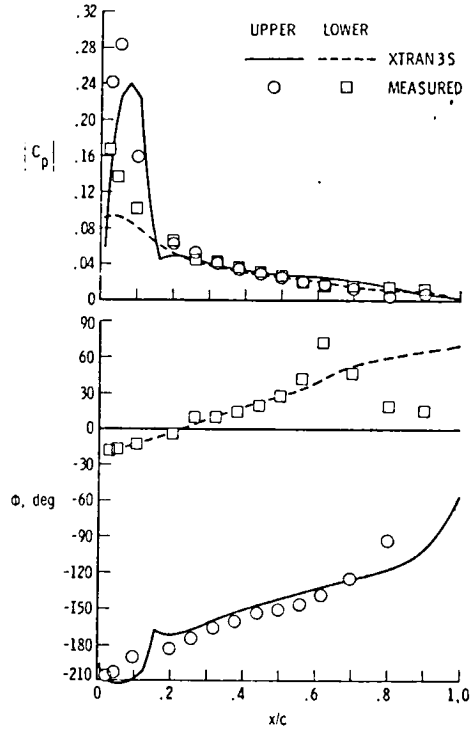

Fig. 13 Comparison of measured and calculated first harmonic unsteady pressure distribution at η = 0.59. M = 0.7, α = 2 deg, f = 10 Hz, Δα = ±1 deg.

Concluding Remarks

Both steady and unsteady aeroynamic data were measured on a rectangular wing with a 12 percent thick supercritical airfoil. The wing was oscillated in pitch to acquire the unsteady data. The purpose of the test was to provide experimental data to assist in the development and assessment of transonic analytical codes. The effect of the wing tip (that is, three-dimensional effects) on the pressure distributions is large. Specifically, the shock location at the outboard sections is considerably farther forward than for inboard sections. Parameters that also have a large effect on the shock strength and location include Mach number and mean angle of attack. Oscillation frequency has a significant effect on the unsteady-pressure magnitudes and phases. Oscillation amplitude affects the unsteady-pressure magnitudes in a linear manner, except at the shock where some non-linearity exists.

Results from the newly-developed XTRAN3S non-linear transonic program and from the linear RHOIV kernel function program were compared to the measured data. The XTRAN3S steady and unsteady results agreed fairly well with measured data at a Mach number of 0.7. It is believed that the inclusion of viscosity in the analysis and use of a finer grid will give

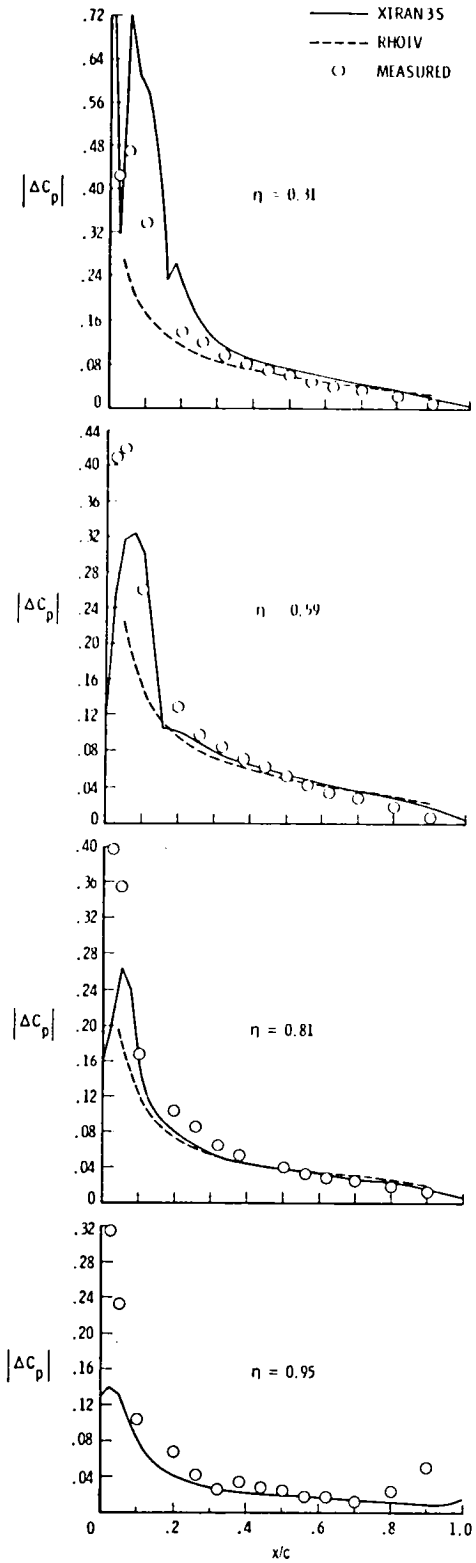

(a) Magnitude.

Fig. 14 Spanwise comparison of measured and calculated unsteady pressure distribution. M = 0.7, α = 2 deg, f = 10 Hz, Δα = ±1 deg.

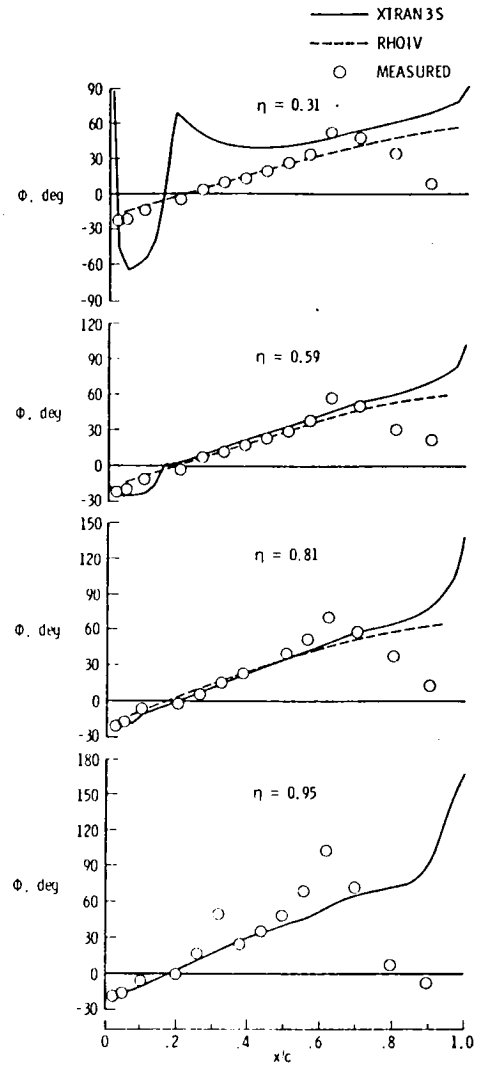

(b) Phase.

Fig. 14 Continued.

better results, particularly at the wing leading edge. The RHOIV unsteady results were in fair agreement, but, of course, the location or strength of the shock was not predicted.

References

[1]Hess, R. W., Wynne, E. C., and Cazier, F. W., Jr., "Static and Unsteady Pressure Measurements on a 50 Degree Clipped Delta Wing at M=0.9," Presented at AIAA/ASME/ASCE/AHS 23rd Structures, Structural Dynamics and Materials Conference, New Orleans, LA, May 10-12, 1982, AIAA Paper No. 82-0686. (Also available as NASA TM 83297, April 1982.)

[2]Sandford, M. C., Ricketts, R. H., Cazier, F. W., Jr., and Cunningham, H. J., "Transonic Unsteady Airloads on an Energy Efficient Transport Wing with Oscillating Control Surfaces," Journal of Aircraft, Vol. 18, No. 7, July 1981.

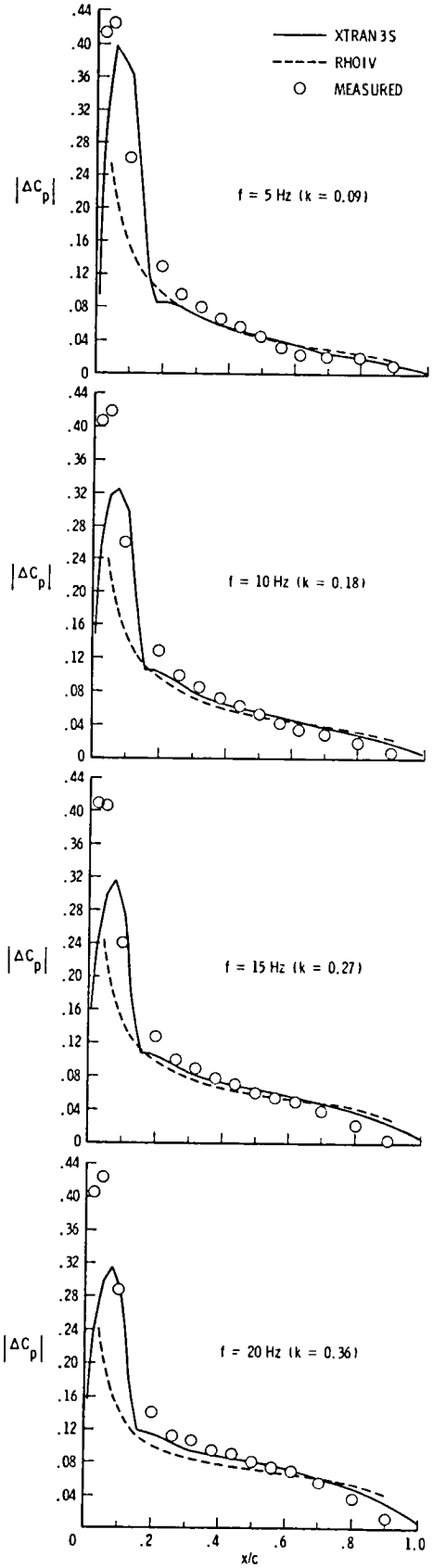

(a) Magnitude.

Fig. 15 Effect-of-frequency comparison at η = 0.59. M = 0.7, α = 2 deg, $\Delta\alpha$ = $\pm$1 deg.

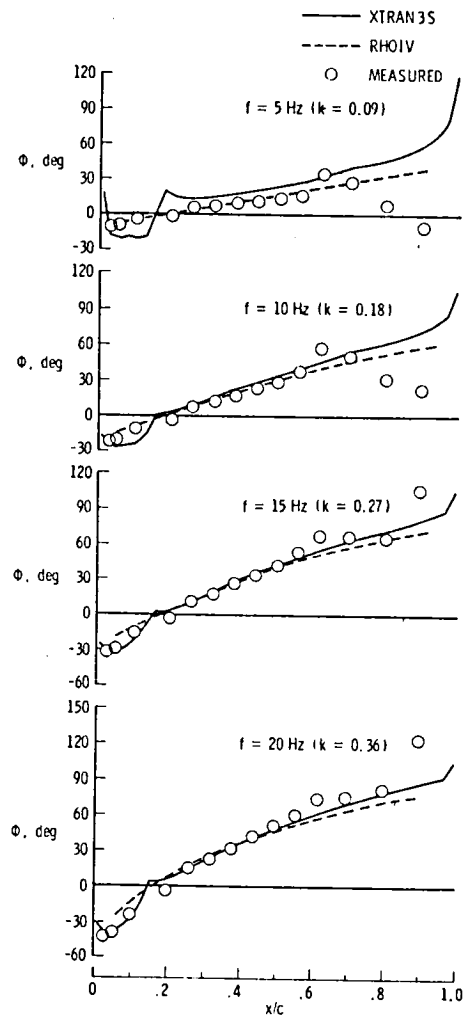

(b) Phase.

Fig. 15 Continued.

[3]Borland, C. J., and Rizzetta, D. P., "Nonlinear Transonic Flutter Analysis," Presented at AIAA Dynamic Specialist Conference, April 9-10, 1981, AIAA-81-0608-CP, April 1981.

[4]Borland, C. J., and Rizzetta, D. P., "Transonic Unsteady Aerodynamics for Aeroelastic Applications - Technical Development Summary." AFFWAL TR 80-3107, Vol. 1, June 1982.

[5]Whitcomb, Richard T., "Review of NASA Airfoils," Presented at the Ninth Congress of the International Council of the Aeronautical Sciences, Haifa, Israel, ICAS Paper No. 74-10, August 1974.

[6]Tijdeman, H., "Investigations of the Transonic Flow Around Oscillating Airfoils," NLRTR 77090 U, National Aerospace Laboratory (Amsterdam), 1977. (Available from DTIC as AD B027 633.)

[7]Cole, Patricia H., "Wind Tunnel Real-Time Data Acquisition System," NASA TM 80081, April 1979.

[8]Seidel, D. A., Bennett, Robert M., and Whitlow, Woodrow, Jr., "An Exploratory Study of Finite Difference Grids for Transonic Unsteady Aerodynamics," Presented at 21st AIAA Aerospace Sciences Meeting, Reno, NV, Jan. 10-13, 1983, AIAA Paper No. 83-0503. (Also available as NASA TM 84583, December 1982.)

[9]Van der Vooren, J., Sloof, J. W., Hizing, G. H., and Van Essen, A., "Remarks on the Suitability of Various Transonic Perturbation Equations to Describe Three-Dimensional Transonic Flow--Examples of Computations Using a Fully-Conservative Rotated Difference Scheme," Symposium Transonicum II, Gottingen, West Germany, Sept. 1975, Proceedings, Springer-Verlag, Berlin, 1976, pp. 557-566.

[10]Redman, M. C., and Rowe, W. S., "Prediction of Unsteady Aerodynamic Loadings Caused by Leading Edge and Trailing Edge Control Surface Motions in Subsonic Compressible Flow - Computer Program Description," NASA CR 132634, 1975.

[11]Bauer, F., Garabedian, P., Korn, D., and Jameson, A., "Supercritical Wing Sections II. Lecture Notes in Economics and Mathematical Systems," M. Beckmann and H. P. Lunzi, eds., Springer-Verlag, c. 1975.

1. Report No.	2. Government Accession No.	3. Recipient's Catalog No.
NASA TM 84616		

4. Title and Subtitle	5. Report Date
TRANSONIC PRESSURE DISTRIBUTIONS ON A RECTANGULAR SUPERCRITICAL WING OSCILLATING IN PITCH	March 1983
	6. Performing Organization Code: 505-33-43-07
7. Author(s): Rodney H. Ricketts, Maynard C. Sandford, David A. Seidel and Judith J. Watson	8. Performing Organization Report No.
	10. Work Unit No.
9. Performing Organization Name and Address: NASA Langley Research Center, Hampton, VA 23665	11. Contract or Grant No.
	13. Type of Report and Period Covered: Technical Memorandum
12. Sponsoring Agency Name and Address: National Aeronautics and Space Administration, Washington, DC 20546	14. Sponsoring Agency Code

15. Supplementary Notes

AIAA Paper #83-0923

This paper was presented at the 24th AIAA/ASME/ASCE/AHS Structures, Structural Dynamics and Materials Conference, May 2-4, 1983, Lake Tahoe, NV.

16. Abstract

Steady and unsteady aerodynamic data were measured on a rectangular wing with a 12 percent thick supercritical airfoil mounted in the NASA Langley Transonic Dynamics Tunnel. The wing was oscillated in pitch to generate the unsteady aerodynamic data. The purpose of the wind-tunnel test was to measure data for use in the development and assessment of transonic analytical codes. The effects on the wing pressure distributions of Mach number, mean angle of attack, and oscillation frequency and amplitude were measured. Results from the newly-developed XTRAN3S program (a non-linear transonic small disturbance code) and from the RHOIV program (a linear lifting surface kernel function code) were compared to measured data for a Mach number of 0.7 and for oscillation frequencies ranging from 0 to 20 Hz. The XTRAN3S steady and unsteady results agreed fairly well with the measured data. The RHOIV unsteady-result agreement was fair but, of course, did not predict shock effects.

17. Key Words (Suggested by Author(s))	18. Distribution Statement
Transonic Aerodynamics Unsteady, Steady Pressures Supercritical Wing Wind-Tunnel Test	Unclassified - Unlimited Subject Category 02

19. Security Classif. (of this report)	20. Security Classif. (of this page)	21. No. of Pages	22. Price
Unclassified	Unclassified	11	A02

For sale by the National Technical Information Service, Springfield, Virginia 22161